

## Some specific Features of the GCR Measurements made by the ATIC Instrument

N.L. Grigorov<sup>a</sup>, Yu.I. Stozhkov<sup>b</sup> and E.D. Tolstaya<sup>a</sup>

(a) Skobeltsyn Institute of Nuclear Physics, Moscow State University, 119992, Moscow, Russia

(b) P.N. Lebedev Physical Institute, Russian Academy of Sciences, Leninsky pros., 53, Moscow, 119991, Russia

Presenter: Yu. Stozhkov (stozhkov@fian.fiandns.mipt.ru), rus-stozhkov-Y-abs2-og11-poster

It is shown that the data published by the ATIC collaboration [2 - 4, 6] are internally controversial. The 'proton' spectrum in reality is the spectrum of particles with  $Z = 1$ . It contains 'additional' particles, imitating protons. If we subtract from  $I_{Z=1}$  the 'additional' particles, we obtain the proton spectrum  $I_p(E)$ . It has a 'knee' at  $E \approx (1 \div 2)$  TeV. Before the 'knee' the spectral index is  $\beta_p = 2.6$  and after it  $\beta_p = 3.0 \div 3.2$ .

The spectrum of GCR protons in the energy range  $\sim 30 \leq E \leq 10^4$  GeV was measured for the first time on the 'PROTON' satellite in 1965-68. It had a 'knee' at  $E \sim 1$  TeV. At lower energies the spectral index was  $\beta_p = 2.6$ , whereas at higher energies it was  $\beta_p = 3.1 \div 3.2$ . Since that time numerous experiments confirmed that at  $E \leq 1$  TeV  $\beta_p = 2.6 \div 2.7$ . For the energy range  $E > 1$  TeV there are no less than 14 direct measurements, out of which only three give  $\beta_p < 3.0$ , whereas all the others give  $\beta_p > 3.0$  (see our paper at this Conference "What is known about the Proton Spectrum in the Energy Range 1  $\div$  40 TeV?"). The mean value of  $\beta_p$ , averaged over all the 14 experiments is  $\langle \beta_p \rangle = 3.05 \pm 0.05$ .

However, the ATIC instrument does not see the 'knee'. Why?

We have made an attempt to answer this question. We compared all the available data on proton spectra and corresponding all-particle spectra measured by the ATIC instrument and published by the present time. At first, we digitized all the spectra and transformed them to the  $E^\beta I$  and  $E^{\beta-1} (dN/d \lg E)$  forms. We also introduced a unit-less value  $M = E^\beta I / \langle E^\beta I \rangle$  or  $M = E^{\beta-1} (dN/d \lg E) / \langle E^{\beta-1} (dN/d \lg E) \rangle$ , where the mean values correspond to the energy range of about (300  $\div$  1000) GeV. The published results of the two ATIC instrument flights after detailed consideration reveal a number of specific features in the experimental data. We will discuss them below.

**Feature 1.** The all-particle spectra in the global flux  $I_{all}^{2\pi}$  (curve 1 in Fig.1) and within the instrument's angular aperture  $I_{all}^\Omega$  (curve 2 in Fig.1) are different [1, 2]. The first spectrum has spectral index  $\beta$  which changes at  $E = 1 \div 2$  TeV by  $\Delta\beta = 0.2 \pm 0.04$ . The second spectrum has  $\beta = \text{const} = 2.6$  up to  $E \approx 10$  TeV.

**Feature 2.** The proton spectra obtained as the difference between the all-particle spectra and the spectra of nuclei with  $Z \geq 2$  are different if we use  $I_{all}^{2\pi}$  and  $I_{all}^\Omega$  values (curves 1 and 2 in Fig. 2). In one case the proton spectrum has a 'knee' at the energy of  $\sim 1$  TeV: before the knee the spectral index is  $\beta_p = 2.6 \div 2.65$ , and after it  $\beta_p = 3.0 \div 3.1$ ; in the other case  $\beta_p = \text{const} = 2.6 \div 2.65$  up to  $E = 6 \div 8$  TeV.

**Feature 3.** The directly measured proton spectrum in the  $M(E)$  representation has the shape of a 'pitcher' (see Fig. 3). Such a spectrum contradicts the X-Ray emulsion chamber measurements.

**Feature 4.** For  $E = (0.1 \div 1)$  TeV the spectrum of the global all-particle flux and the spectrum in the angular

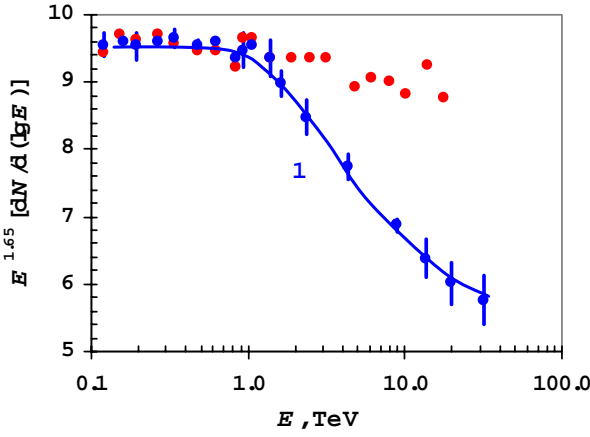


Figure 1.

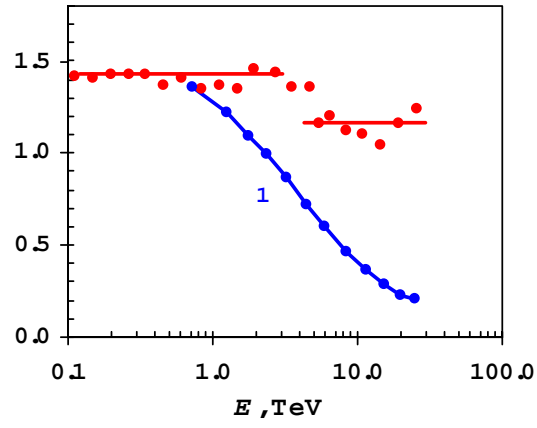


Figure 2.

aperture of the instrument coincide after normalization of the intensities. For  $E > 1$  TeV the intensity of the all-particle flux within the angular aperture is larger than the intensity of the global flux. (see Fig. 1).

**Feature 5.** Comparison of the spectra, measured using the whole matrix  $100 \times 100$  cm<sup>2</sup> (intensity  $I_{100}$ ) and part of the matrix  $80 \times 80$  cm<sup>2</sup> (intensity  $I_{80}$ ), permits to determine the intensity of particles passing through the peripheral part of the matrix  $I_{per}$ . It turns out that  $I_{per} > I_{80}$ , and the difference increases with increasing  $E$ .

The above listed features look like contradictions in the experiment itself. We believe that there is a certain physical process, which explains all these contradictions. Let us consider this process. Due to the large error  $\sigma$  in retracing the coordinates of the primary particle and recording of backscatter particles by the charge detectors the recording of ‘additional’ particles, i.e. particles arriving outside the angular aperture of the instrument, is possible (in detail, see [5]). The ATIC instrument satisfies the requirements necessary for recording ‘additional’ particles. Keeping in mind feature 5, it can be supposed, that the flux of particles with  $Z = 1$ , recorded by the instrument, consists of protons with intensity  $I_p(E)$  and ‘additional’ particles with  $I_{ad}(E)$ , i.e.

$$I_{z=1}(E) = I_p(E) + I_{ad}(E). \quad (1)$$

The intensity of ‘additional’ particles  $I_{ad}$  should be proportional to the intensity of cosmic rays, which produce them, and also proportional to the probability that a sensor within area  $S = (6\sigma)^2$  will be triggered by backscatter particles. This probability is proportional to the intensity of backscatter  $I_{bs}$  and area  $S$ .

Therefore, we can write  $I_{ad} \sim I_{CR} \cdot I_{bs} \cdot S$ . Since  $I_{CR} \sim E^{-\beta}$ ,  $I_{bs} \sim E^\alpha$  [6],  $S = 36\sigma^2$ , then

$$I_{ad} = BE^{-\beta} E^\alpha \sigma^2 = BE^{-(\beta-\alpha)} \sigma^2 \quad (2)$$

We will assume that the proton spectrum has a ‘knee’, i.e. can be described as  $I_p(E) = CE^{-\beta} f(E)$ , where

$$f(E) = \left[ 1 + \left( \frac{E}{a} \right)^2 \right]^{-0.25} \cdot \left[ 1 + 0.3 \frac{(E/a)^2}{1 + (E/a)^2} \right]. \quad (3)$$

Multiplying  $I_{z=1}$  by  $E^\beta$ , we obtain  $E^\beta I_{z=1} = E^\beta I_p + E^\beta I_{ad} = Cf(E) + BE^\alpha \sigma^2(E)$

At  $E \geq 1$  TeV  $\sigma(E) = \text{const} = 3.5$  cm [6]. Therefore, assuming  $\beta = 2.6$ ;  $\alpha = 0.5$ , we finally obtain

$$E^{2.6} I_{Z=1} = C[f(E) + D(E/0.3)^{0.5}] \quad (4)$$

In this representation  $D$  is the fraction of ‘additional’ particles at  $E = 0.3$  TeV. In the global flux they are responsible for about 40% of all the events. Therefore, the global flux should have the spectral index  $\beta_{all} = 0.4\beta_p + 0.6\beta_z$ . The proton spectrum has a ‘knee’, i.e.  $\beta_p = \beta_z$  in the energy range  $E < a$  and  $\beta_p = \beta_z + \Delta\beta \approx \beta_z + 0.5$  in the range  $E > a$ . Nuclei with  $Z \geq 2$  have a purely power law spectrum with  $\beta_z \approx 2.6$ . In the energy range  $E < a$   $\beta_p = \beta_z$ ,  $\beta_{all} = \beta_z = 2.6$ . When  $E > a$   $\beta_p = \beta_z + 0.5$  and  $\beta_{all} = \beta_z + 0.4 \cdot 0.5 \approx \beta_z + 0.2 = 2.8$ . The global all-particle flux, measured by the ATIC instrument, has exactly such parameters [1].

The all-particle flux within the angular aperture of the instrument consists of the fluxes of nuclei and particles with  $Z = 1$ . Multiplying  $I_{all}^\Omega$  by  $E^{2.6}$ , we obtain  $E^{2.6}I_{all}^\Omega = E^{2.6}I_{z=1} + E^{2.6}I_{z \geq 2}$ . Here  $E^{2.6}I_{z \geq 2} = \text{const}$ , therefore, the form of the  $E^{2.6}I_{all}^\Omega$  spectrum is determined by the form of the  $E^{2.6}I_{z=1}$  function, i.e. the spectrum of particles with  $Z = 1$ .

In order to investigate how well expression (4) describes the spectrum of particles with  $Z = 1$ , first of all, we investigated the repeatability of the published data. In order to do this the proton spectra in [2, 3] and the proton spectrum obtained from the difference of  $I_p = I_{all}^\Omega - I_{z \geq 2}$  were expressed in terms of the unit-less value  $M(E)$  (see above) and plotted in the Fig. 3. It can be seen, that the spectra of the first and second flights coincide. They also coincide with  $I_p = I_{all}^\Omega - I_{z \geq 2}$ . After that using expression (4) we calculated the expected spectrum for  $Z = 1$  particles for  $a = 1.5$  TэВ и  $D = 0.057$  and, expressing it in the  $M(E)$  form, also plotted it in Fig. 3 as a curve 1. This curve coincides well with the experimental spectrum, which has a specific feature -  $E^{2.6}I_{z=1} = \text{const}$  up to energies  $E \cong 6 \div 8$  TeV. Therefore,  $E^{2.6}I_{all}^\Omega$  is also constant up to these energies. It is actually observed in the experiment (see Fig. 1). In Fig. 3 some of the spectra  $M$  are represented as a function of energy deposit  $E_d$ , and others as a function of the particle energy  $E$ . This incorrectness has been corrected by multiplying by 2.5, i.e.  $E = 2.5 \cdot E_d$ . All the three spectra, expressed in terms of  $E$ , were averaged. We have been convinced that the averaged spectrum coincides with the data in Fig. 3.

Therefore, it can be seen, that the assumption that the flux of particles with  $Z = 1$ , measured by the ATIC instrument, besides protons contains their imitations in the form of ‘additional’ particles fully explains the previously mentioned (1- 4) features.

‘Additional’ particles are produced by all high energy GCR particles, which enter the detector of energy through the sides of the instrument. Therefore, they will create an excessive intensity at the peripheral parts of the instrument.

From the obvious expression  $N_{100} = N_{80} + N_{per}$  by algebraic transformations we obtain:

$$\frac{I_{per}}{I_{80}} = \left( \frac{I_{100}}{I_{80}} - \frac{G_{80}}{G_{100}} \right) / \left( 1 - \frac{G_{80}}{G_{100}} \right) \quad (5)$$

Here  $N_{100}$ ,  $N_{80}$ ,  $N_{per}$  - are the numbers of particles, recorded by the whole matrix (100x100 cm<sup>2</sup>), its portions (80x80 cm<sup>2</sup>) and periphery part, and  $G$  are the corresponding geometry factors. From Fig.3 it can be seen that at  $E > 10$  TeV  $(M_{100}/M_{80}) = (I_{100}/I_{80}) > 1$ . Introducing  $(I_{100}/I_{80}) > 1$  into (5), we obtain  $(I_{per}/I_{80}) > 1$ . We can see that at the periphery of the instrument the intensity really is larger than in the centre. In other words, the fact of ‘additional’ particle recording by the ATIC instrument is an experimental reality.

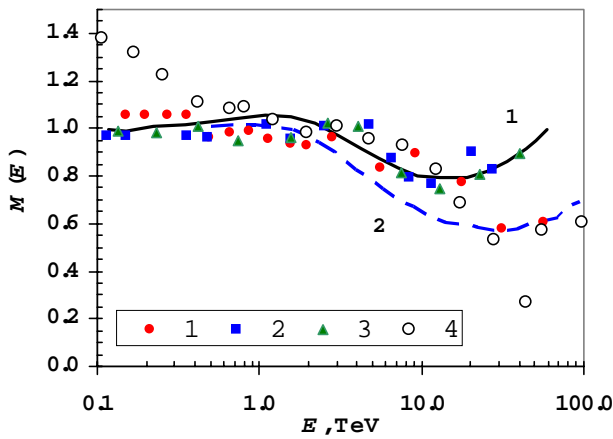


**Figure 3.** Proton spectra expressed in unit-less value  $M(E)$  (see text). Spectra 1, 2, 3 were measured by the silicon matrix with dimensions  $100 \times 100 \text{ cm}^2$ , spectrum 4 – by the matrix with dimensions  $80 \times 80 \text{ cm}^2$ . The curves are the spectra of particles with  $Z = 1$ , calculated using expression (4) at  $a = 1.5 \text{ TeV}$  and  $D = 0.057$  (curve 1) and  $D = 0.03$  (curve 2).

## Conclusions

1. The ATIC instrument records not the proton spectrum, but the spectrum of particles with  $Z = 1$ .
2. The measured spectrum of particles with  $Z = 1$  consists of two spectra: the spectrum of GCR protons and the spectrum of ‘additional’ particles.
3. ‘Additional’ particles are generated inside the instrument itself by GCR particles, arriving outside the aperture of the instrument (they are recorded as particles with  $Z = 1$ ), due to significant errors in reconstructing the trajectory of primary particles and recording of backscatter particles by the charge detector (silicon matrix).
4. ‘Additional’ particles strongly distort the proton spectrum. If we subtract the contribution of ‘additional particles’ from the spectrum of particles with  $Z = 1$ , the remaining proton spectrum has a ‘knee’ at  $E \approx (1.5 \div 2) \text{ TeV}$ . Before the ‘knee’  $\beta_p \approx 2.6$ . After the ‘knee’  $\beta_p \approx 3.0 \div 3.2$ . This spectrum with a ‘knee’ is in good agreement with the proton spectrum, obtained from the global all-particle spectrum, measured by the same instrument.
5. The use of the silicon matrix as a charge detector, has experimentally proved, that decreasing of the sensor dimensions, without corresponding decrease in the error  $\sigma$  does not protect the instrument from backscatter influence.

## References

- [1] Yu. Stozhkov, N. Grigorov. Short communication in physics FIAN, No. 5, 3 (2004).
- [2] H.S. Ahn et al., 28<sup>th</sup> ICRC, Japan (2003), 1853 .
- [3] H.S. Ahn et al., 28<sup>th</sup> ICRC, Japan (2003), 1833.
- [4] V. Zatsepin et al., 28<sup>th</sup> ICRC, Moscow (2004), 1102.
- [5] N. Grigorov, G. Kahidze, E. Tolstaya, PTE, No. 1, 1 (2004) (in Russian)..
- [6] V. Zatsepin et al., 28<sup>th</sup> ICRC, Japan (2003), 1861.